

Supplementary Material

1 CONVERGENCE

To ensure the RANS simulations have reached a steady state we check if they have converged. After they have converged, they will be used to initialize LES. This study is performed for the wide 3D domain with an orientation of 90° . The variation of the velocity field from the last 40 time frames of the RANS simulation is analyzed. The standard deviation is found to be a maximum of 0.06% for the velocity and 2.1% for the turbulent kinetic energy, both measured in front of the solar array. The higher percentage of turbulent kinetic energy is attributed to the relatively large increase at the beginning of the array, where the value is lower in the wake. The defined time resolution for RANS is deemed sufficient for fully developing the flow.

2 GRID ASSESSMENT

The grid is assessed using narrow 3D LES simulations. Since the narrow 3D grid is the same as the cross-section in the xz -plane for the wide 3D simulations, the narrow 3D grid results are applicable. In LES, the concept of grid convergence is controversial unless the cut-off length scale is completely decorrelated from the computational grid. In this study, the LES results from two different grid sizes are time-averaged and then compared to assess grid size sensitivity. The two grid resolutions are referred as the coarse grid resolution and the used grid resolution, being 1.5 times finer than the coarse grid.

The time-averaged velocity fields for a coarse grid and the used grid are plotted in Fig. 1 (xy -plane) and Fig. 2 (xz -plane). The LES results are averaged over the last 100 time frames (see Sec. 6 for the validation of this time range). The used grid with the finer resolution revealed more flow details, including smaller eddies, but showed similar vertical wake penetration compared to the coarse grid resolution. The xz -flow fields for both grids look similar. The xy -flow field shows some differences between $x=0.1L$ and $2.2L$, but they become more similar further downstream. The coarse grid does not show any oscillations after $4.4L$, which could indicate that the grid is too coarse to dissipate the eddies to smaller scales.

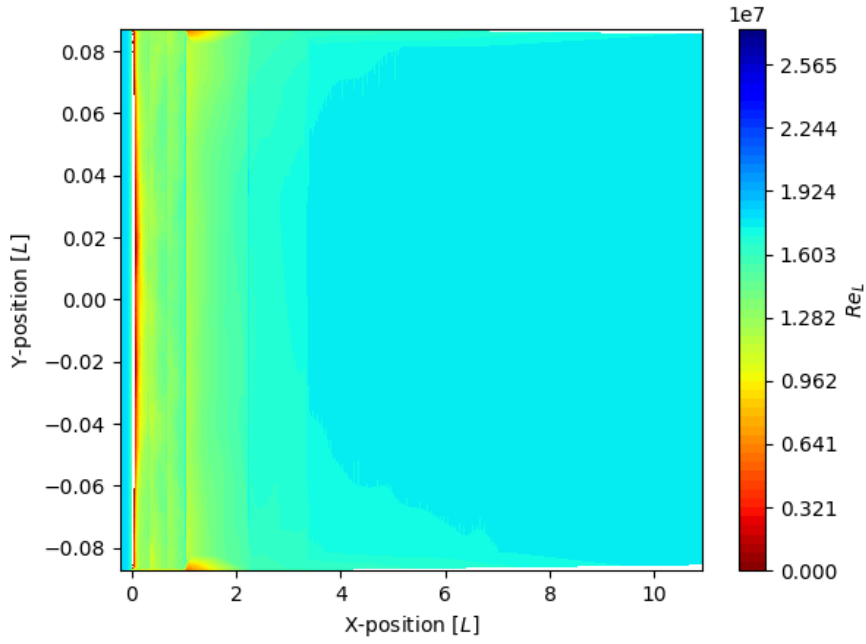


Figure 1a. The coarse grid resolution.

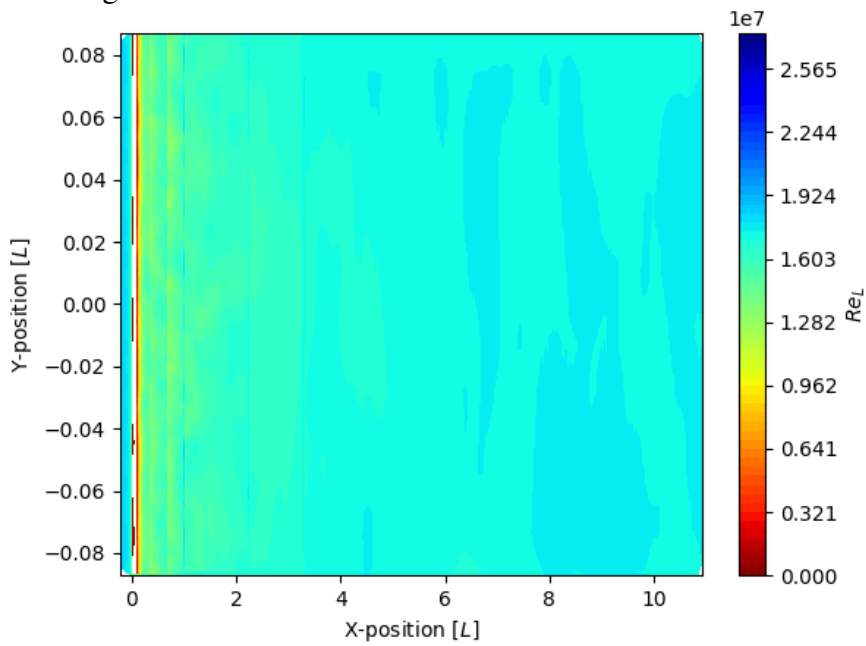


Figure 1b. The used grid resolution 1.5 times finer than the coarse grid.

Figure 1. The xy -plane at a depth of $\frac{1}{3}d$ for the time-averaged narrow 3D LES simulation over the last 100 time frames for a coarse and used grid resolution. The contours represent the velocity flow field in space indicated by Re_L .

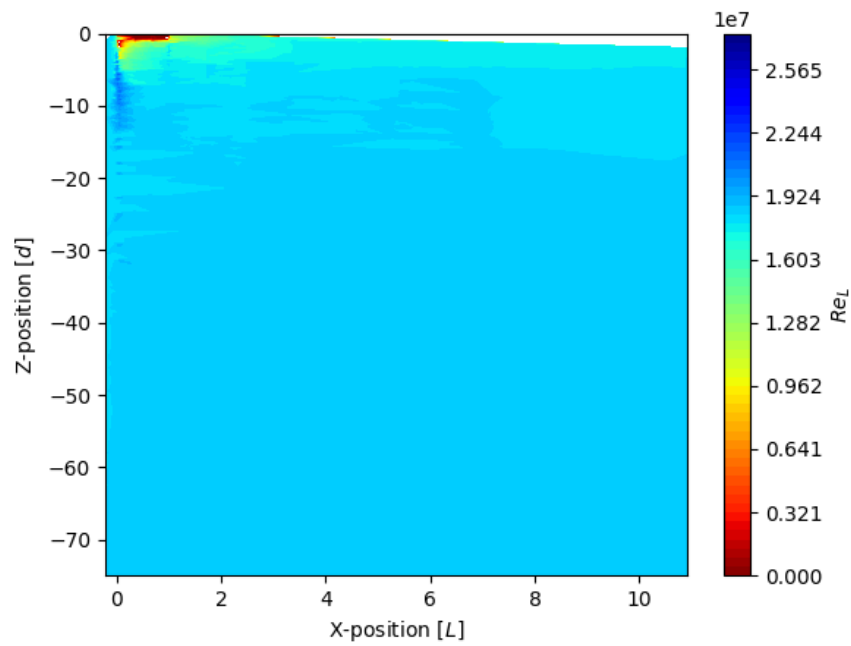


Figure 2a. The coarse grid resolution.

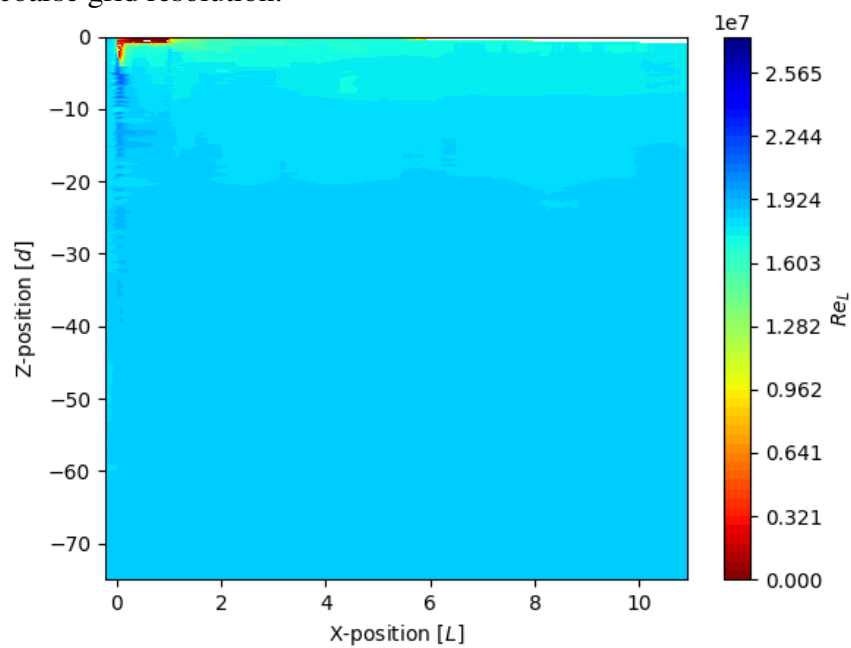


Figure 2b. The used grid resolution 1.5 times finer than the coarse grid.

Figure 2. The xz-plane of the time-averaged narrow 3D LES simulation over the last 100 time frames for a coarse and used grid resolution. The contours represent the velocity flow field in space indicated by Re_L .

3 TURBULENCE MODELLING & COURANT NUMBER

In Fig. 3 the velocity profiles beneath the array at $0.10L$ and $0.16L$ are plotted for the narrow 3D case with $Re_L=1.83e7$ for different turbulence models in OpenFOAM. The simulations are performed with a Courant number restriction of 1 unless mentioned otherwise and are averaged over the last 100 time frames.

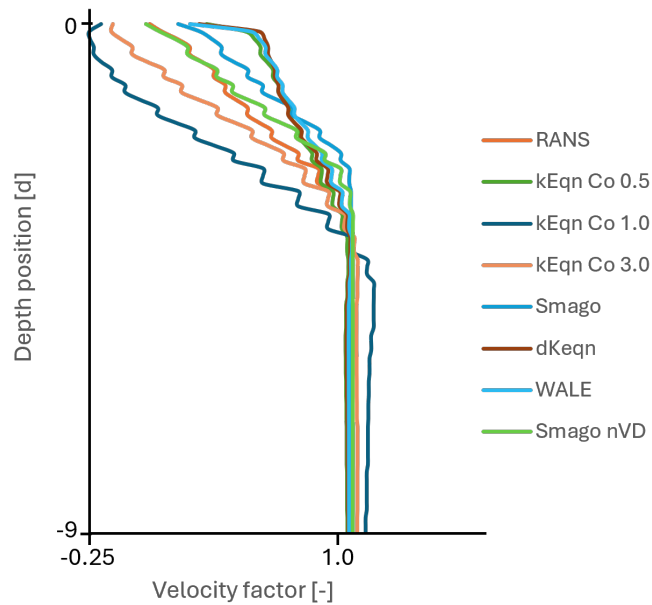


Figure 3a. At a length position of $0.10L$.

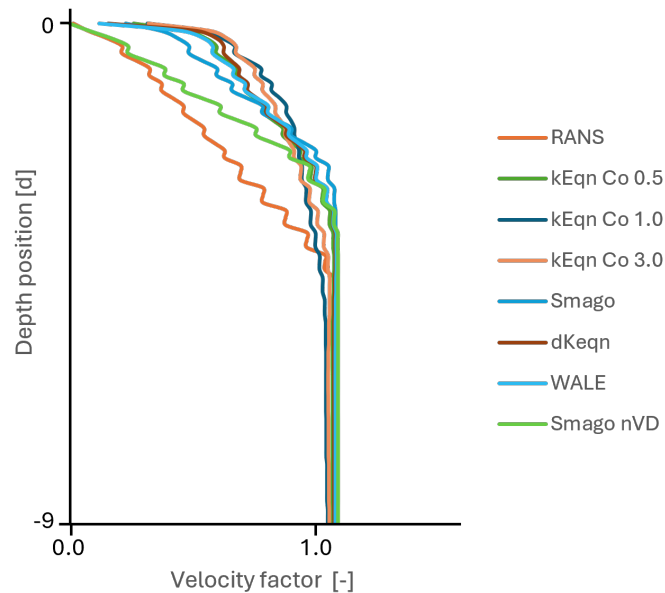


Figure 3b. At a length position of $0.16L$.

Figure 3. The velocity profile over the depth for the narrow 3D case for different turbulence models.

Several key conclusions can be drawn about the performance of various turbulence models and their effects on boundary layer characteristics. The Smagorinsky model without van Driest damping (Smagorinsky nVD in Fig. 3) tends to overestimate dissipation and shear at the plate. When compared to RANS, Smagorinsky produces results that are more similar to RANS.

The Courant number has a notable influence on the results, particularly for the k equation (KEqn). At Courant numbers 1 and 3, the transition to the turbulent region is found to occur later than predicted by boundary layer theory, around $Re_x=2.2e6$. However, the k equation at a Courant number of 0.5, the dynamic k equation (dKEqn), and the WALE model exhibit similar behavior, with a transition occurring around $Re_x=1e6$. For computational efficiency reasons, the dynamic k equation (dKEqn) is used in this article with a Courant restriction of 1.

4 WALL FUNCTION

To reduce computational costs, a wall function is applied at the bottom of the solar array. A wall function can be applied when the turbulent scales are small enough such that they exhibit predictable, isotropic behavior. A commonly used wall function is the kqR wall function (from the OpenFOAM software package), which provides a simple wrapper around the zero-gradient condition. This wall function can be used for the turbulent kinetic energy and the Reynolds stress tensor fields.

A high Reynolds wall function is suitable when the y^+ value is in the log-layer between 20-30 and 200-300. For a case like this, it is challenging to manage this for all grid cells. A wall function is suitable when the pressure gradient hardly changes, a condition that is not met in regions of flow separation, where the wall function can introduce errors. The decision is made to use low Reynolds modeling, with y^+ values lower than 5 in the area of interest. This approach is chosen because, for LES, there seems no suitable wall functions available in the log-layer (high Reynolds approach).

The results are illustrated in Fig. 4 for the buffer layer for one time instance with LES and an orientation of 0° . A horizontal contour at the depth of the solar array in the wide 3D domain is shown. It was experienced that the RANS gives an average y^+ more than three times higher than LES. The presence of y^+ values in the buffer layer (Fig. 4) and logarithmic layer (log-law layer) are minimal, making the choice of using low Reynolds modelling ($y^+ < 5$) suitable for the used grid resolution.

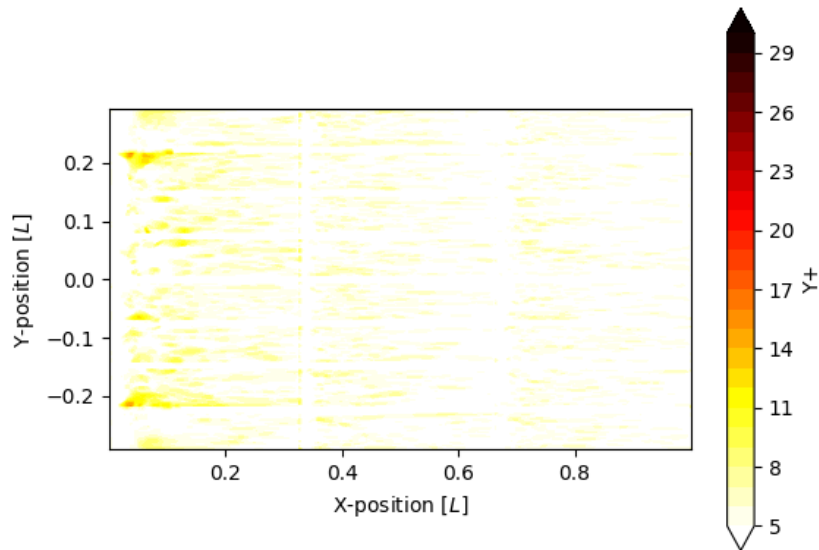


Figure 4. The y^+ value for the bottom view of the solar array in the buffer layer. The LES results are not averaged over time.

For a low y^+ value in the viscous sublayer, the wall-function effect should be rather small. However, the orientation could affect the y^+ value due to flow amplification. The y^+ criterion based on the LES results are given in Tab. S1. The values are a range because LES is time dependent; the average remains similar and y^+ is just below 5. At the front where flow separation occurs, it is slightly higher, indicating that the flow separation might not be correctly determined. However, in the area of interest where boundary layer development occurs, the criteria are met.

Table S1. Wall criteria based on wide 3D LES results for different rotations.

| Orientation [°] | y_{min}^+ | y_{max}^+ | y_{avg}^+ |
|-----------------|-------------|-------------|-------------|
| 0.0 | 0.2 | 24-39 | 4.7 |
| 22.5 | 0.3-0.4 | 22-26 | 5.0 |
| 45.0 | 0.2-0.3 | 22-25 | 5.5 |
| 67.5 | 0.2-0.3 | 25-30 | 4.8 |
| 90.0 | 0.2 | 24-34 | 4.2 |

The difference between applying the high Reynolds wall function or the low Reynolds wall functions on the velocity probes beneath the array and the wake is shown in Fig. 5 for the wide 3D LES case with 67.5° orientation. The effect of the wall functions is only visible near the plate from $0d$ to $3d$. Applying the high Reynolds wall functions resulted in a slightly thicker boundary layer.

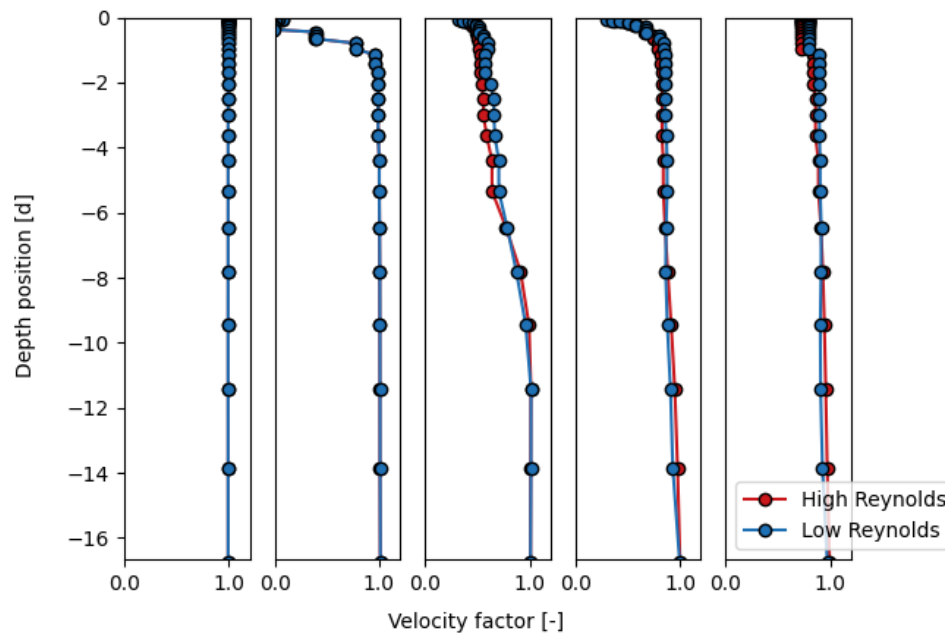


Figure 5a. At width position of $0.45W$.

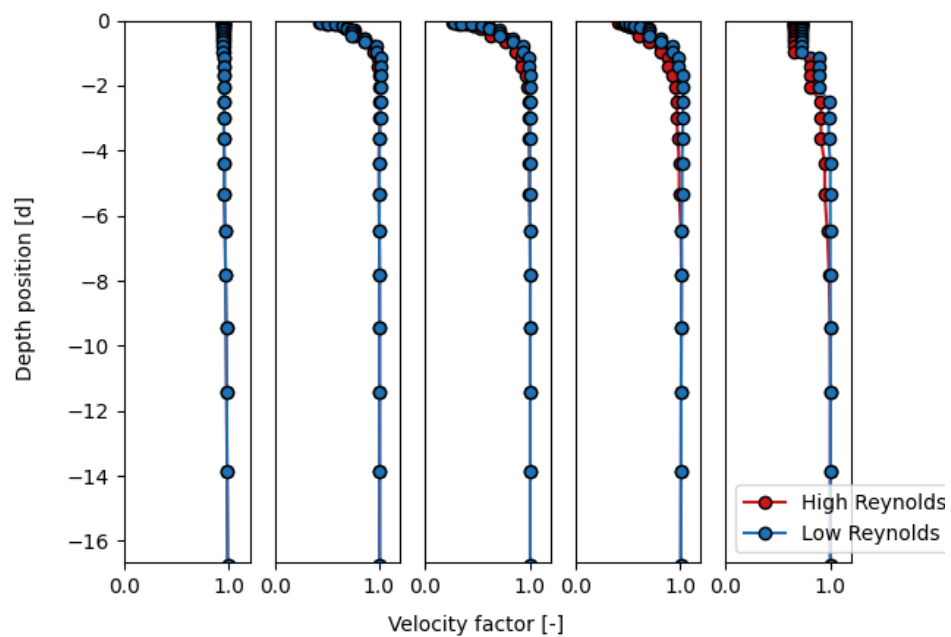


Figure 5b. At width position of $-0.45W$.

Figure 5. The velocity profile over the depth with α equal to 67.5° and averaged over 100 time frames. Five locations in the x-direction are provided starting at the front of the array: 0.03 , 0.3 , 0.5 , 0.7 , and $0.97L$.

A comparison test was conducted between rough high-Reynolds wall functions, accounting for marine growth of 50 mm, and low-Reynolds wall functions, using the narrow 3D case. The key difference in grid resolution is that prism layers are omitted for the rough high-Reynolds wall function to maintain a cell size comparable to the roughness. However, this approach resulted in y^+ values reaching up to 1200, which exceeds the log-layer range ($y^+ < 300$) where the high-Reynolds wall function is valid. Consequently, the boundary layer thickness—measured as wake depth—is larger beneath the array when using the rough high-Reynolds wall function, though it matches the wake depth in the wake region. Despite potential uncertainties arising from different grid resolutions and the application of wall functions affecting flow separation, the low-Reynolds wall function with a grid incorporating prism layers was chosen. This configuration led to the largest wake length.

5 COVERAGE OF TURBULENT KINETIC ENERGY SPECTRUM

A rule of thumb is that LES should capture at least 80% of the large turbulent eddies, as small-scale eddies exhibit isotropic behavior and are thus more amenable to modeling by the turbulence model. To reduce computational costs, RANS simulations can provide a good preliminary assessment of whether the grid is sufficiently fine for LES. In this section, the RANS simulation is performed for an array with an orientation of 67.5° , after the flow has approached a steady state (with a maximum deviation of 1%) in time. The following formula is used for the RANS simulation

$$f = \frac{l_0}{\Delta^{1/3}} = \frac{\nu_t}{C_\mu \sqrt{k}} > 5, \quad (\text{S1})$$

where C_μ is a constant with a value of 0.09, k and ν_t the turbulent kinetic energy and eddy viscosity, and Δ the grid volume. This equation indicates whether a LES simulations would be able to solve at least 80% of the turbulent eddies.

The result for f is shown in the top plots of in Fig. 6 for two different depth positions. The value for f is above 5 in the area of interest. However, at the front of the array it is lower which could indicate that flow separation is not correctly modelled. Based on the top plots we conclude that the grid was sufficient to test for LES and look if 80% is resolved.

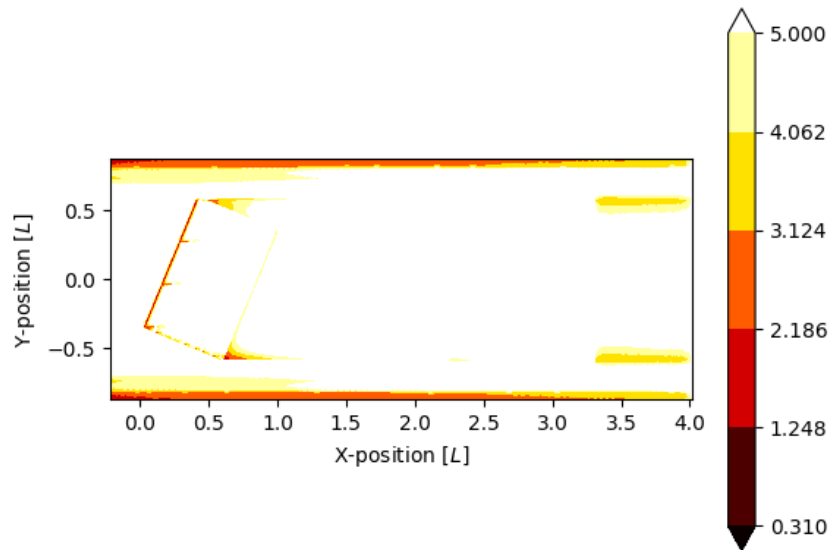


Figure 6a. At depth position of $1\frac{1}{3}d$.

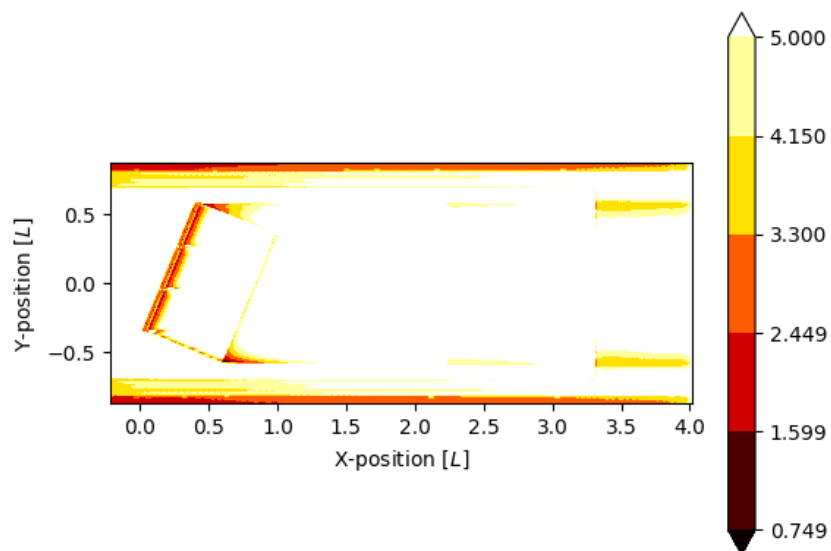


Figure 6b. At depth position of $2\frac{2}{3}d$.

Figure 6. The xy-contour planes showing the criteria for ‘f’ for the orientation of 67.5° and current velocity of $Re_L=1.83e7$.

After performing the LES simulation of this case, Fig. 7 is made. The ratio of resolved turbulent kinetic energy over the total turbulent kinetic energy (resolved plus modelled) is illustrated. Especially for a x smaller than $2.2L$, the eddies seem to be resolved for 80%. However, for x larger than $3.3L$ the resolved turbulence becomes in average lower than 80% and is less trustworthy.

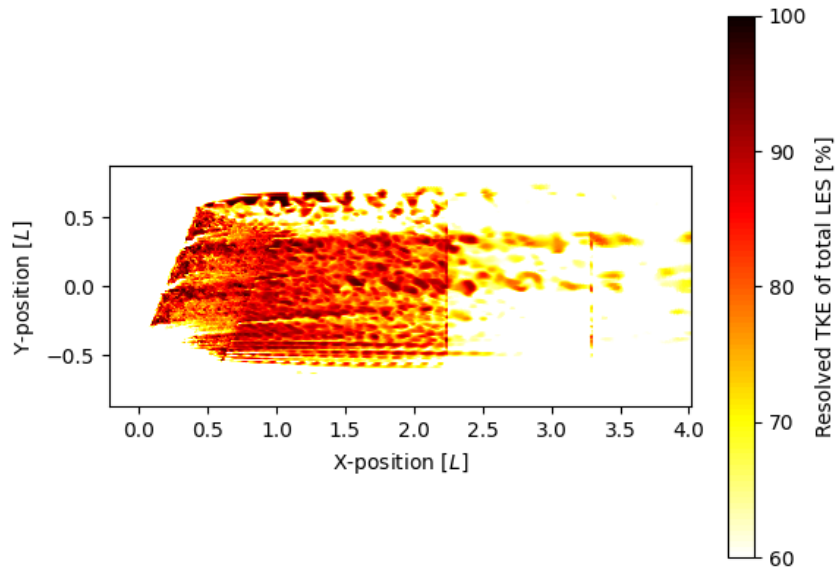


Figure 7a. At depth position of $1\frac{1}{3}d$.

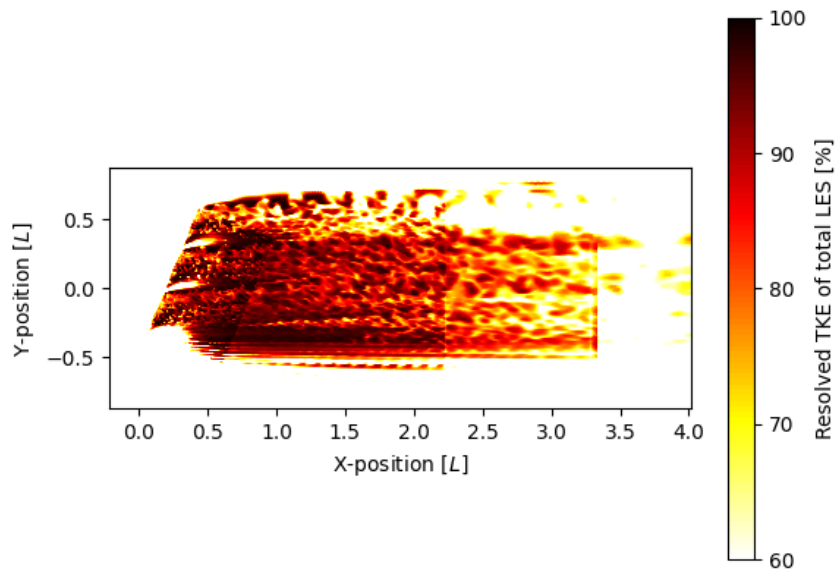


Figure 7b. At depth position of $2\frac{2}{3}d$.

Figure 7. The xy-contour planes showing the percentage of resolved turbulent eddy scales for the orientation of 67.5° and current velocity of $Re_L=1.83e7$.

We conclude that the grid is sufficient, weighing against computational costs, for modelling the boundary layer development, the area of interest, but less for detecting the flow separation. Grid refinement is not performed, up to at least 40 million cells, because of the high computational costs. The less-resolved turbulence for x larger than $3.3L$ needs to be accounted for in further analyses because at this distance mixture can be underestimated. That's why the TUDFLOW3D were performed with a denser grid in the wake of the array.

6 TIME COVERAGE 3D LES

The final assessment is the convergence of LES in time. The LES simulations must run for a duration sufficient to ensure that the flow field, initially derived from RANS, is fully displaced out of the numerical domain and that flow features have developed. A time range must be identified where the LES results remain consistent for accurate wake size analysis. Figure 8 shows the time development of the velocity probes over increments of 50 frames. Time frame 0 corresponds to the point when the flow has completed one pass through the domain. The criterion used for convergence is that the maximum change in results should be below 1%. This condition is met during the last 100 time frames (200-300) of the simulation, which are used for the analysis in this article.

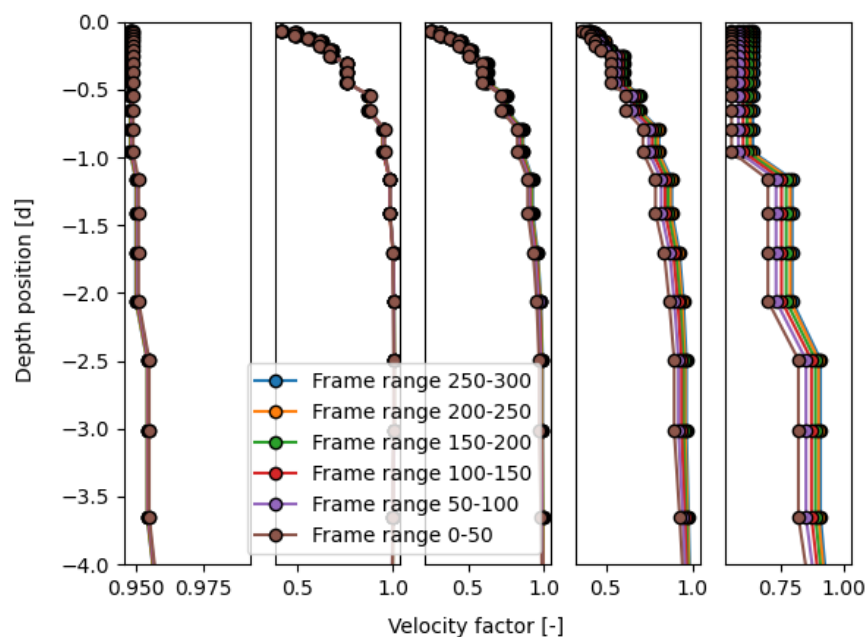


Figure 8. Velocity probes with LES signal averaged per 50 frames. The location is at a width of $-0.45W$ beneath the array for an orientation of 67.5° .